Regulation of photosystem I light harvesting by zeaxanthin

Matteo Ballottari[a], Marcelo J. P. Alcocer[b,c], Cosimo D'Andrea[b,c], Daniele Viola[c], Tae Kyu Ahn[d,e,f], Annamaria Petrozza[b], Dario Polli[b,c], Graham R. Fleming[d,f], Giulio Cerullo[c], and Roberto Bassi[a,1]

[a]Department of Biotechnology, University of Verona, I-37134 Verona, Italy; [b]Center for Nanoscience and Technology, Italian Institute of Technology, Polytechnic University of Milan, 20133 Milan, Italy; [c]Institute for Photonics and Nanotechnology, National Research Council, Department of Physics, Polytechnic University of Milan, 20133 Milan, Italy; [d]Physical Biosciences Division, Lawrence Berkeley National Laboratory, Berkeley, CA 94720; [e]Department of Energy Science, Sungkyunkwan University, Suwon 440-746, Korea; and [f]Department of Chemistry, University of California, Berkeley, CA 94720

Edited by Elisabeth Gantt, University of Maryland, College Park, MD, and approved May 2, 2014 (received for review March 7, 2014)

In oxygenic photosynthetic eukaryotes, the hydroxylated carotenoid zeaxanthin is produced from preexisting violaxanthin upon exposure to excess light conditions. Zeaxanthin binding to components of the photosystem II (PSII) antenna system has been investigated thoroughly and shown to help in the dissipation of excess chlorophyll-excited states and scavenging of oxygen radicals. However, the functional consequences of the accumulation of the light-harvesting complex I (LHCI) proteins in the photosystem I (PSI) antenna have remained unclarified so far. In this work we investigated the effect of zeaxanthin binding on photoprotection of PSI–LHCI by comparing preparations isolated from wild-type *Arabidopsis thaliana* (i.e., with violaxanthin) and those isolated from the *A. thaliana* nonphotochemical quenching 2 mutant, in which violaxanthin is replaced by zeaxanthin. Time-resolved fluorescence measurements showed that zeaxanthin binding leads to a previously unrecognized quenching effect on PSI–LHCI fluorescence. The efficiency of energy transfer from the LHCI moiety of the complex to the PSI reaction center was down-regulated, and an enhanced PSI resistance to photoinhibition was observed both in vitro and in vivo. Thus, zeaxanthin was shown to be effective in inducing dissipative states in PSI, similar to its well-known effect on PSII. We propose that, upon acclimation to high light, PSI–LHCI changes its light-harvesting efficiency by a zeaxanthin-dependent quenching of the absorbed excitation energy, whereas in PSII the stoichiometry of LHC antenna proteins per reaction center is reduced directly.

photosynthesis | xanthophylls | violaxanthin de-epoxidase | photobleaching

In eukaryotic photosynthetic organisms, photosystem I (PSI) and photosystem II (PSII) comprise a core complex hosting cofactors involved in electron transport and an outer antenna system made of light-harvesting complexes (LHCs): Lhcas for PSI and Lhcbs for PSII. The core complexes bind chlorophyll a (Chl a) and β-carotene, whereas the outer antenna system, in addition to Chl a, binds chlorophyll b (Chl b) and xanthophylls. Despite their overall similarity, PSI and PSII differ in the rate at which they trap excitation energy at the reaction center (RC), with PSI being faster than PSII (1–9). They also differ in their structure (10–12). PSI is monomeric and carries its antenna moiety on only one side as a half-moon–shaped structure whose size is not modulated by growth conditions (13, 14). PSII, on the other hand, is found mainly as a dimeric core surrounded by an inner layer of antenna proteins (Lhcb4–6) and an outer layer of heterotrimeric LHCII complexes (Lhcb 1–3) whose stoichiometry varies depending on the growth conditions (7, 12, 13, 15). Acclimation to high irradiance leads to a lower number of trimers per PSII RC accompanied by loss of the monomeric Lhcb6. These slow acclimative responses regulate the excitation pressure on the PSII RC, preventing saturation of the electron transport chain (16) and the oxidative stress in high light (HL), leading to photoinhibition. The response to rapid changes in light level is managed by turning on some photoprotective mechanisms, such as the nonphotochemical quenching (NPQ) of the excess energy absorbed by PSII (16), which is activated by the acidification of the thylakoid lumen and protonation of the trigger protein PsbS or LhcSR. Low luminal pH also activates violaxanthin de-epoxidase (VDE), catalyzing the de-epoxidation of the xanthophyll violaxanthin to zeaxanthin (17, 18), a scavenger of reactive oxygen species (ROS) produced by excess light (9, 13). Zeaxanthin also enhances NPQ, as observed in vivo by a decrease of PSII fluorescence (19). The short-term effects of exposure to HL on PSI have been disregarded thus far. Because of its rapid photochemistry, PSI shows low fluorescence emission, implying a low ^{1}Chl* concentration and a low probability that chlorophyll triplet states will be formed by intersystem crossing. This characteristic suggests that the formation of oxygen singlet excited states ($^1O^*_2$) is reduced and that NPQ phenomena in photoprotection are less relevant in PSI (20, 21). Nevertheless, several reports have shown that, especially in the cold (22–29), PSI can exhibit photo-inhibition, with its Lhca proteins being the primary target (24, 30). Upon synthesis in HL, zeaxanthin binding could be traced to two different types of binding site. One, designated "V1," is located in the periphery of LHCII trimers (31–33). The second, designated "L2," has an inner location in the dimeric Lhca1–4 and the monomeric Lhcb4–6 members of the LHC family (34–37). Experimental determination of the efficiency of the violaxanthin-to-zeaxanthin exchange yielded a maximal score in the Lhca3 and Lhca4 sub-

Significance

Chloroplasts are particularly prone to photooxidative damage, and carotenoids play a key role in photoprotection. Under excess light conditions, plants accumulate a carotenoid, zeaxanthin, involved in multiple photoprotection events. Although the function of zeaxanthin in photosystem II (PSII) has been investigated thoroughly, its role in photosystem I (PSI) had not been identified. In this work we report a zeaxanthin-dependent regulation of PSI functional antenna size in *Arabidopsis thaliana*. We identified a zeaxanthin-dependent quenching process coupled to improved photostability of PSI, as measured in isolated complexes and leaves. We show that, similar to its action in PSII, zeaxanthin binding to components of PSI leads to the formation of carotenoid radical cations, quenching a fraction of the excitation energy absorbed.

units (24, 25). Interestingly, Lhca1/4 and Lhca2/3 are bound to the PSI core as dimers that can be isolated in fractions identified as "LHCI-730" and "LHCI-680," respectively, both accumulating zeaxanthin to a de-epoxidation index of ~0.2 (20, 38). Lhca3 and Lhca4 carry low-absorption-energy chlorophyll forms known as "red forms" (39, 40) that are responsible for the red-shifted PSI emission peak at 730–740 nm at 77 K. The molecular basis for red forms is an excitonic interaction of two chromophores: chlorophylls 603 and 609 located a few angstroms from the xanthophyll in site L2, which can be either violaxanthin or zeaxanthin depending on light conditions (41, 42). It is unclear whether the binding of zeaxanthin to the PSI–LHCI complex has specific physiological function(s) or is simply a result of its common origin with Lhcb proteins.

The goal of this study was to understand whether zeaxanthin plays a role in PSI–LHCI photoprotection. To investigate the role of zeaxanthin bound to Lhca proteins, we analyzed the changes in antenna size and Chl a fluorescence dynamics in PSI supercomplexes binding either violaxanthin or zeaxanthin. We found a zeaxanthin-dependent regulation of PSI antenna size and an enhanced resistance to excess light upon zeaxanthin binding. These results show that dynamic changes in the efficiency of light use and in photoprotection capacity are not exclusive to PSII, as previously thought; instead, eukaryotic photosynthetic organisms modulate the function of both photosystems in a coordinated manner.

Results

Zeaxanthin Accumulation Improves PSI Photoprotection in Vivo. To verify that zeaxanthin has a photoprotective role for PSI–LHCI, we measured the activity of the RC of PSI (P700) in leaves of *Arabidopsis thaliana* following HL treatment (1,000 $\mu mol \cdot m^{-2} \cdot s^{-1}$) at 4 °C. The activity of the PSI RC ($P700 > P700^{+}$) was measured by detecting the loss of absorption at 705 nm following a saturating light pulse as previously described (43). We compared the WT leaves with the nonphotochemical quenching 1 (*npq1*) mutant leaves, which lacks VDE activity and cannot form zeaxanthin upon light stress (44). In our experimental conditions, the conversion of violaxanthin to zeaxanthin in WT leaves yielded de-epoxidation indices of 0.3 and 0.5 after 30 min and 90 min of illumination, respectively. In Fig. 1*A* we report P700 activity: Although it remained essentially constant in WT leaves, a small reduction being detected only at 90 min, P700 activity in *npq1* leaves was reduced significantly after 30 min and decreased further (to a 25% loss) upon 90-min treatment. These results suggest that zeaxanthin accumulation in thylakoid membranes prevented PSI photoinhibition, thus allowing sustained P700activity.

Photoprotection in Purified PSI–LHCI. It can be asked whether the photoprotective effect of zeaxanthin is caused directly by its binding to the PSI–LHCI complex or is an indirect effect from PSII–LHCII, where it can be found bound, decreasing the production of reactive oxygen species (ROS) which diffuse from grana to PSI in stroma membrane domains (45). To identify the photoprotective effects specifically associated with PSI–LHCI, we extended the experiments to isolated PSI–LHCI. PSI–LHCI complexes with or without zeaxanthin were purified by sucrose gradient ultracentrifugation of thylakoids solubilized with dodecyl-maltoside (46) from the *A. thaliana* nonphotochemical quenching 2 (*npq2*) mutant, which lacks violaxanthin and constitutively accumulates zeaxanthin (44), or from dark-adapted WT *A. thaliana*, which contains violaxanthin but not zeaxanthin. Pig-ment analyses of the isolated PSI–LHCI complexes are reported in Table S1. P700 activity was measured in isolated PSI–LHCI

upon illumination with HL (1,000 $\mu mol \cdot m^{-2} \cdot s^{-1}$) at 4 °C. The results are reported in Fig. 1*B*. The light-induced formation of P700+ was similar in both PSI–LHCI complexes before HL treatment. However, when the actinic light was switched on, the activity declined faster in the violaxanthin-binding sample than in the zeaxanthin-binding sample. In the first 30 min, the loss of P700+ was twice as strong in the PSI–LHCI from WT *A. thaliana* as in the PSI–LHCI from *A. thaliana npq2*. At longer treatment times the difference declined; however, even after 2 h of illumination violaxanthin-binding PSI–LHCI had 20% less activity than zeaxanthin-binding PSI–LHCI (Fig. S1). Finally, we measured the loss of chlorophyll absorption caused by photobleaching during the light treatment (Fig. 1*C*) and found less photobleaching of PSI–LHCI in the presence of zeaxanthin, as is consistent with of zeaxanthin' having a photoprotective role.

Localization of Zeaxanthin Within PSI–LHCI. Previous reports demonstrated that zeaxanthin can be found in PSI–LHCI and is bound by LHCI proteins (20, 36, 38). To localize zeaxanthin within the PSI–LHCI supercomplex, we fractionated it into its two components, PSI-core and LHCI, by a procedure reported previously (47, 48). Fig. S2 shows the sucrose gradient separation pattern of the dissociation products from PSI–LHCI isolated from dark-adapted WT *A. thaliana* and *npq2* leaves and from WT *A. thaliana* leaves stressed for 30 min at HL (hereafter referred to as "stressed WT") to induce zeaxanthin accumulation. Fraction 1 previously has been attributed to pigments known as "gap pigments" at the interface between the LHCI and PSI-core

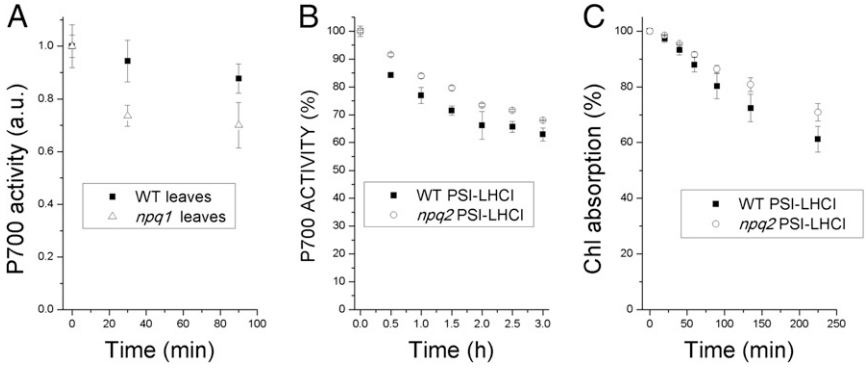

Fig. 1. Photoprotective role of zeaxanthin bound to PSI. (*A*) P700 activity measured as P700 oxidation on whole leaves from WT and *npq1* plants exposed to strong light (2,000 $\mu mol \cdot m^{-2} \cdot s^{-1}$) for 30 min and 90 min. (*B*) P700 activity measured as P700 oxidation on PSI–LHCI complexes isolated from WT and *npq2* upon illumination with strong light (1,000 $\mu mol \cdot m^{-2} \cdot s^{-1}$). (*C*) Photobleaching curves of PSI–LHCI complexes isolated from WT and *npq2* plants measured as the decrease of 600- to 750-nm integrated chlorophyll absorption.

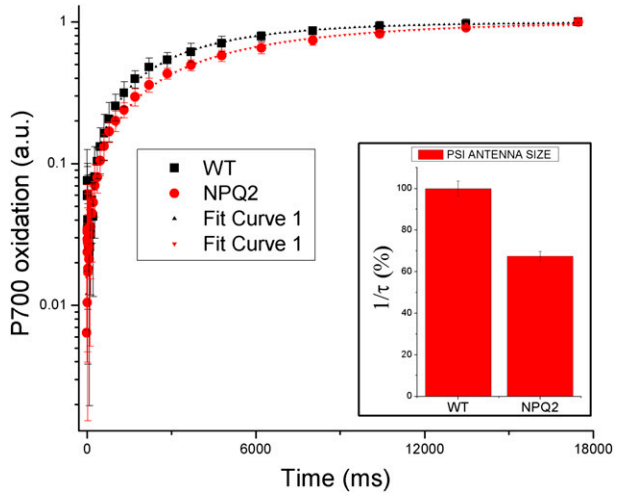

Fig. 2. Functional antenna size in PSI–LHCI supercomplexes. The antenna size in WT and *npq2* mutant PSI–LHCI was determined by measuring the kinetics of P700 oxidation upon illumination with 12 μmol·m^{-2}·s^{-1}. The kinetics curve was fitted with a monoexponential curve characterized by a time constant τ (τ_{WT} = 5.59 s and τ_{NPQ2} = 3.76 s). (*Inset*) Estimation of PSI–LHCI antenna size as 1/τ normalized to 100 in the case of PSI–LHCI WT.

moieties of the supercomplex (10). In addition, pigments originally bound to pigment proteins and freed by the dissociation procedure also might be present in this fraction. Fraction 2 is composed of LHCI complexes, and fraction 3 is composed of the PSI-core. Fractions 4 and 5, with higher molecular density, originate from PSI-core complexes that still retain portions of Lhca proteins. Pigment analysis (Table S2) of the different fractions reveals that some zeaxanthin can be found in all fractions from either *npq2* or stressed WT samples but is highly enriched in fractions 1 and 2. In particular, we quantified the chlorophyll content in the different fractions in the gradient and used these data to calculate the distribution of zeaxanthin within the fractions (Table S2). Of the total zeaxanthin, 44% was found in fraction 2 (LHCI), 37% in fraction 1 (gap pigments + freed pigments), 5% in fraction 3 (PSI-core), and 6–12% in fractions 4 and 5. Values in the two zeaxanthin-binding samples (*npq2* and stressed WT) were similar. A similar distribution was found for violaxanthin in WT PSI–LHCI. These results suggest that the violaxanthin/zeaxanthin exchange in PSI–LHCI occurs predominantly in LHCI and in the gap pigments.

Functional Characterization of Zeaxanthin-Binding PSI–LHCI Complexes. To investigate the mechanism by which zeaxanthin increases photoprotection in PSI–LHCI, we measured the spectroscopic properties of PSI–LHCI and LHCI isolated from WT and *npq2 A. thaliana* plants as described in ref. 48. Absorption spectra of PSI–LHCI complexes binding violaxanthin or zeaxanthin are reported in Fig. S3. Small differences are detectable in the Soret and in the Q_Y region, resulting from zeaxanthin absorption at 500–510 nm and a slight increase in Chl b content in the presence of zeaxanthin (peaks at 470 and 650 nm). Similar results were found for LHCI from WT and *npq2 A. thaliana* (Fig. S3 *B* and *C*). Fluorescence emission spectra of PSI–LHCI and LHCI at 77 K instead showed increased amplitude of the 730-nm vs. the 685-nm peaks in the *npq2* sample as compared with WT. This finding suggests that zeaxanthin binds to the L2 site in proximity to chlorophylls 603 and 609, because the interaction between chlorophylls 603 and 609 originates the red forms (41). To investigate further the effect of zeaxanthin binding to Lhca proteins, we measured the stoichi-ometry of PSI-core complex vs. LHCI in WT and *npq2* PSI–LHCI by SDS/PAGE and Coomassie blue staining, as previously reported (48). As shown in Fig. S4 and as is consistent with previous work (13, 48, 49), no significant changes in the amount of Lhca proteins per core complex could be detected when comparing WT and *npq2* samples. We then determined the functional antenna size of PSI–LHCI in WT and *npq2* samples. To do so we measured the rate of P700+ formation under limiting light (μmol·m^{-2}·s^{-1}), which is inversely related to the functional antenna size of PSI–LHCI (14). Fig. 2 shows the kinetics of P700 oxidation by plotting the P700 activity as a function of time. P700 kinetics clearly are slower for *npq2* PSI–LHCI than for WT. Kinetics were fitted with monoexponential functions, and the associated time constants τ were used to calculate the size of the functional antenna (expressed as 1/τ) in PSI–LHCI samples. As reported in Fig. 2, the presence of zeaxanthin induced a decrease of the size of the functional PSI–LHCI antenna by ~30%.

Time-Resolved Fluorescence Analysis of PSI–LHCI, LHCI, and PSI-Core Samples. The changes in functional antenna size detected in the absence of biochemical differences in the stoichiometry of pigment proteins suggest that the differences between WT and *npq2* samples might be functional. To evaluate any influence of zeaxanthin on the migration of excitation energy to the RC (1–5), time-resolved fluorescence measurements were performed on isolated PSI–LHCI supercomplexes. Broadband fluorescence decay kinet-ics was measured with a streak camera detector in the 600–800 nm wavelength range (Fig. S5). Previous kinetics studies on PSI showed predominantly fast fluorescence decay within 500 ps, although a long-lived component (with a time constant from 700 ps to a few nanoseconds) was identified in all the different prepara-tions measured (1–6, 50, 51). This long-lasting component was ascribed to contaminants such as disconnected chlorophylls or poorly connected antenna proteins. Recently, however, Jennings and coworkers (3) suggested the presence of an intrinsic long-lasting component of PSI deriving from a fraction of associated LHCI with a slow energy transfer to the PSI-core complex. We measured the kinetics of PSI–LHCI fluorescence decay using two different observation windows, one in the time range of ~200 ps and another up to 10 ns, with indicative corresponding time resolution of 3 and 100 ps, respectively, to estimate both short-and long-lasting decay components properly. Fig. 3 reports the fluorescence decay kinetics extracted from maps of PSI–LHCI in

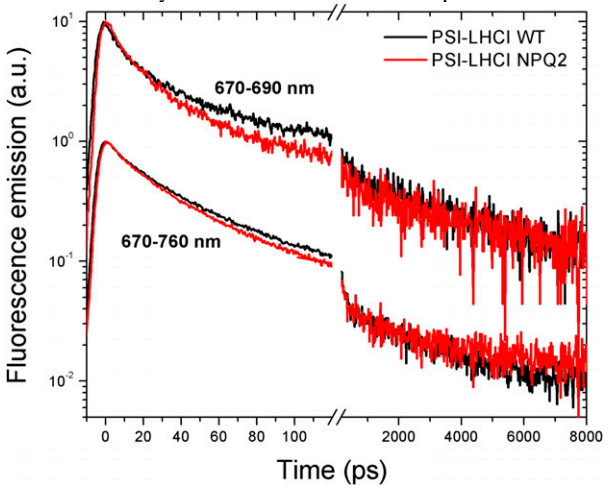

Fig. 3. Fluorescence decay dynamics of PSI–LHCI supercomplexes. Fluorescence decay dynamics were extrapolated from measurements of Streak camera imaging. Streak camera images were integrated in the spectral ranges of 670–760 and 670–690 nm as indicated in the figure. Excitation was performed at 440 nm.

the time range of 0–20 ps, integrated over the spectral range of 670–760 nm and over the restricted range of 670–690 nm corresponding to the peak of fluorescence emission. In both cases decay kinetics are clearly faster in presence of zeaxanthin, especially in the 670–690 nm range, where the contribution of antenna proteins is more evident when PSI–LHCI fluorescence is measured at room temperature (52). A global analysis fitting procedure was applied to analyze fluorescence decay kinetics (53). Briefly, the wavelength–time 2D fluorescence maps were fitted using the sum of four terms, each being the product of a 1D exponential decay function in time with a 1D spectrum (called "decay-associated spectrum," DAS). In this manner, the exponential decay constants were assumed to be independent of wavelength. This procedure allowed the measured fluorescence maps to be decomposed into four contributions, each describing the fluorescence spectrum associated with a specific decay time. In particular this fitting procedure was applied to the time range of 0–200 ps, when most of the emitted fluorescence decays. The longer exponential function, with a nanosecond time constant, was estimated properly by fitting the dataset for the 10-ns time range and was fixed by fitting the time range of 0–200 ps. To analyze the PSI–LHCI data properly, fluorescence decay maps in the 600- to 800-nm range were obtained similarly for isolated LHCI and PSI-core complexes (Fig. S5). Extracted DAS are reported in Fig. 4.

i) In PSI-core samples, fluorescence kinetics are dominated by a 13-ps decay component with spectrum peaking at 689 nm for both WT and *npq2* samples (red curves in Fig. 4 *C* and *D*), usually associated with bulk inner antenna chlorophylls of PSI-core complexes (3–5, 54, 55). Additional components identified include a 5- to 6-ps positive/negative component representing the energy equilibration between the bulk pigments and the low-energy forms associated with the PSI-core (55, 56) and a 58-ps (*npq2*) to 65-ps (WT) component characterized by a peak at 689 nm and a red-shifted shoulder at ~720 nm, which has been associated with the presence of red-shifted forms in the core (4). Finally, a 2-ns contribution having very small amplitude was identified in the PSI-core, likely caused by low-level contamination from disconnected Lhca proteins in the preparation. No major differences between WT and *npq2* samples could be detected in either

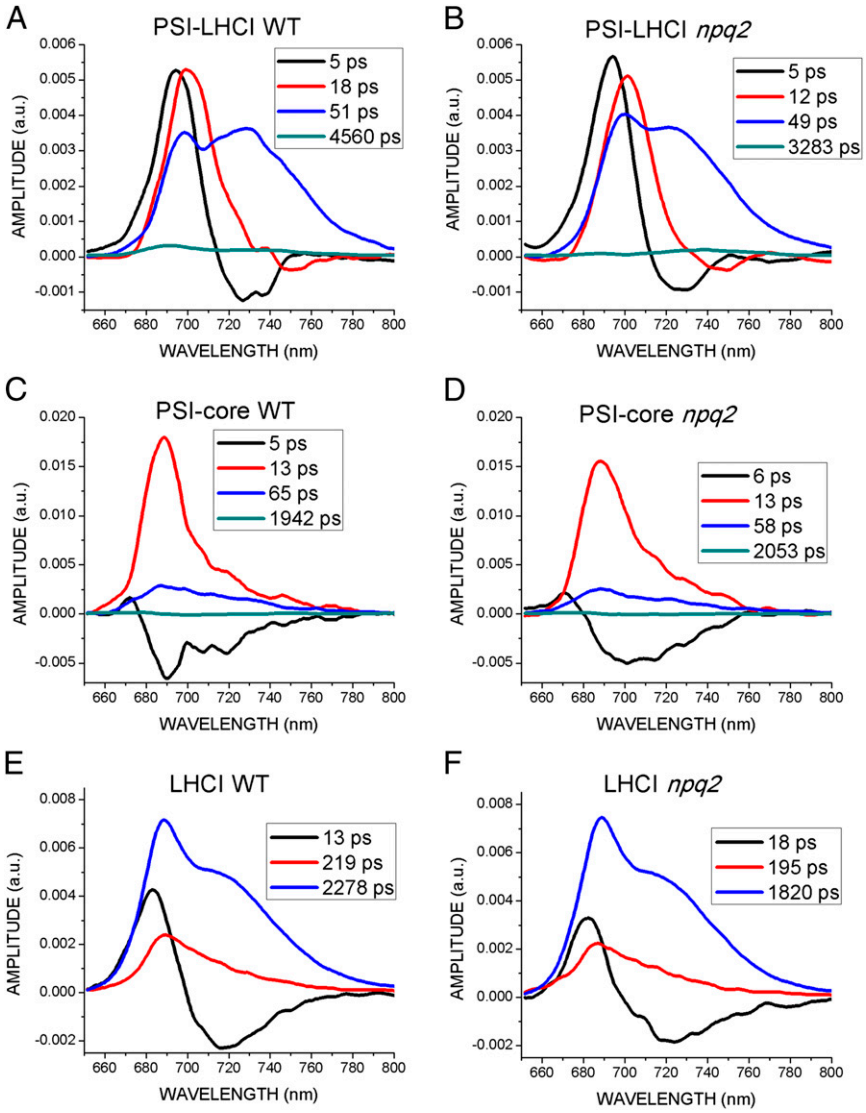

Fig. 4. DAS of PSI–LHCI, PSI-core, and LHCI samples. Streak camera results reported in Fig. 3 were analyzed in terms of global fitting at the different wavelengths. The DAS obtained are reported for PSI–LHCI (*A* and *B*), PSI-core (*C* and *D*), and LHCI (*E* and *F*). The time constant associated with each DAS is indicated in the figure. Errors of time constants and amplitudes are less than 5% ($n = 3$).

time constants or spectral shapes of the DAS. This finding is consistent with the binding of Chl a and β-carotene, but not zeaxanthin, to this complex.

ii) In LHCI samples, the positive-to-negative energy transfer component is slowed to 13 ps in WT and to 18 ps in *npq2*, indicating a general reorganization of the pattern of excitation energy transfer when the pigment-binding proteins are in de-tergent, leading to a slower energy reequilibration kinetics (4). The dominant decay component in LHCI can be described by a single exponential with a 2.3-ns time constant in WT that is reduced to 1.8 ns in presence of zeaxanthin (*npq2*), suggesting the activation of some dissipation mechanisms in presence of zeaxanthin. The spectrum of this component is characterized by a main peak at 690 nm and a red-shifted shoulder at ~720 nm in both samples. A third, minor, ~200-ps component pres-ent in both samples is slightly faster in *npq2* samples, with a peak at 690 nm, and a less evident >700-nm contribution. The different components of LHCI fluorescence decay kinet-ics have been associated with different conformations of the Lhc proteins (57, 58).

iii) In the PSI–LHCI supercomplexes, four components were needed for the deconvolution of decay kinetics, with time constants of 5 ps, 18–12 ps, 50 ps, and 3–4 ns, respectively. The 5-ps energy transfer component is present in both WT and *npq2* PSI–LHCI with similar DAS, showing greater amplitude of the positive contribution when compared with the data from PSI-core samples. The next fastest component was slower in WT PSI–LHCI (18 ps) than in PSI-core (13 ps) samples and showed a red shift from 690 nm to 700 nm (Fig. S6*A*). This result indicates that this 18-ps DAS is dominated by fast excitation energy transfer from the outer, red-shifted LHCI proteins to the inner PSI-core bulk chlorophylls. Interestingly, this component was faster in the presence of zeaxanthin, with a time constant of 12 ps, very close to the 13 ps of the isolated PSI-core, but still peaked at 700 nm. This result suggests that the presence of zeaxanthin in the PSI–LHCI complex induces the rapid dissipation of a fraction of the excitation energy absorbed in LHCI. Consistently, the 12-ps DAS of the *npq2* sample had a reduced 720- nm contribution compared with the 18-ps DAS of the WT sample (Fig. S6*A*), suggesting a reduced contribution from the red-shifted outer antennas. The longer ~50-ps DAS identified in both WT and *npq2* samples was charac-terized by two spectral components at 700 and 725 nm (Fig. 4 *A* and *B*). This component is the red-most DAS in PSI–LHCI and is dominated by fluorescence emission from the LHCI moiety of the supercomplex. In presence of zeaxan-thin, the amplitude of the 725-nm peak is clearly reduced compared with the 700-nm peak (see also Fig. S6*B*), sug-gesting that the excitation energy associated with LHCI is reduced, as is consistent with zeaxanthin-dependent dissipa-tion activity in LHCI. The longest decay component of PSI–LHCI has been measured as 4.5 ns in WT and as 3.3 ns in *npq2* samples (Fig. 4 *A* and *B*). This component, which contributes only 3.9% to the DAS of WT PSI–LHCI and 2.4% to the DAS of *npq2*, is rather different in the two samples, with an increased contribution at 740 nm in pres-ence of zeaxanthin (Fig. S6*C*). Previously, this contribution was ascribed to contaminants, such as free pigments, PSII complexes, or poorly connected LHCI antenna proteins. However, the presence of a 740-nm emission peak in both the WT and *npq2* samples suggests instead that it derives from a population of LHCI proteins poorly transferring to PSI-core. When calculating the average fluorescence life-time (τ_{AV}) of PSI–LHCI, this long-lasting component usu-ally is not considered. τ_{AV} is a value that allows calculation of the effective trapping time across the PSI emission band (52). The results, reported in Fig. 5, demonstrate that the

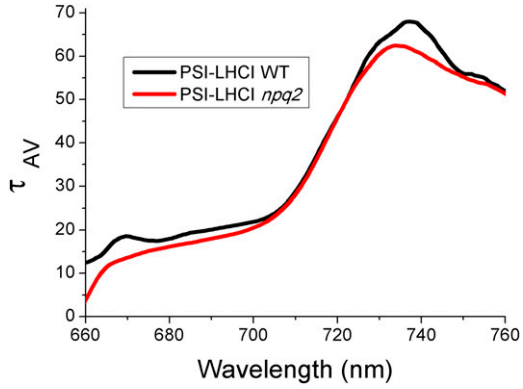

Fig. 5. Trapping time of WT and *npq2* PSI–LHCI. Fluorescence average lifetime (τ_{AV}) was used to calculate the trapping time at the different wavelengths of WT and PSI–LHCI complexes. τ_{AV} was calculated as the average of the different time constants reported in Fig. 4 weighted by the amplitudes of the exponentials at the different wavelengths.

τ_{AV} clearly is reduced in zeaxanthin-binding PSI–LHCI at wavelengths below 700 nm and in the far-red region above 730 nm. Fluorescence emission in these regions is influenced more by LHCI than by the PSI-core. Taken together these results suggest that the presence of zeaxanthin induces a partial quenching of excitation energy absorbed by LHCI but does so only when it is connected to the PSI-core.

Zeaxanthin-Dependent Charge Transfer Quenching in Lhca4. The nature of the zeaxanthin-dependent dissipative mechanism in LHCI was investigated using a simple and homogeneous system consisting of isolated Lhca4, i.e., the LHCI component with the red-most fluorescence emission forms. Lhca4 proteins with either zeaxanthin or violaxanthin, in addition to Chl a, Chl b, and lutein, were prepared as previously reported (59) (Table S3). The most noticeable spectroscopic features in LHCI proteins are the red-shifted forms originating from a charge-transfer state between two closely interacting chromophores, chlorophylls 603 and 609 (41, 60). To investigate the possible influence of the red forms on quenching, we analyzed a mutant version of Lhca4 carrying an N47H (Lhca4-NH) mutation that suppresses the red forms (29). The fluorescence quantum yields of the WT and N47H Lhca4 proteins binding either lutein + violaxanthin (Lhca4-NH-LV) or lutein + zeaxanthin (Lhca4-NH-LZ) are reported in Table S4. The reductions in fluorescence yield caused by zeaxanthin and by the red forms were 14–19% and 33%, respectively, as is consistent wit ref. 60. Previous work with Lhcb4–6 proteins has shown that zeaxanthin binding to site L2 results in the formation of a zeaxanthin radical cation and quenching (59, 61). Therefore we carried out transient absorption measurements at 980 nm as reported previously (59, 61). The results are reported in Fig. 6. In both Lhca4-WT-LV and Lhca4-WT-LZ the 980-nm transient absorption kinetics was character-ized by a rapid rise followed by a slower decay, whereas the am-plitude of the signal increased in presence of zeaxanthin. The zeaxanthin-dependent component, obtained by subtracting the Lhca4-WT-LV trace from the Lhca4-WT LZ trace, can be fitted by a single exponential rise with a 6-ps time constant and an exponential decay with a 167-ps time constant. In the absence of red forms (Lhca4-NH-LZ), the amplitude of the 980-nm tran-sient absorption kinetics was strongly reduced. In Lhca4-NH-LV, a pure decay was observed. Again, the difference, Lhca4-NH-LZ minus Lhca4-NH-LV, can be described with a 6-ps rise and 100-ps decay. These results suggest that Lhca4 in detergent solution undergoes quenching of chlorophyll-excited states through the formation of zeaxanthin radical cations and that the efficiency of

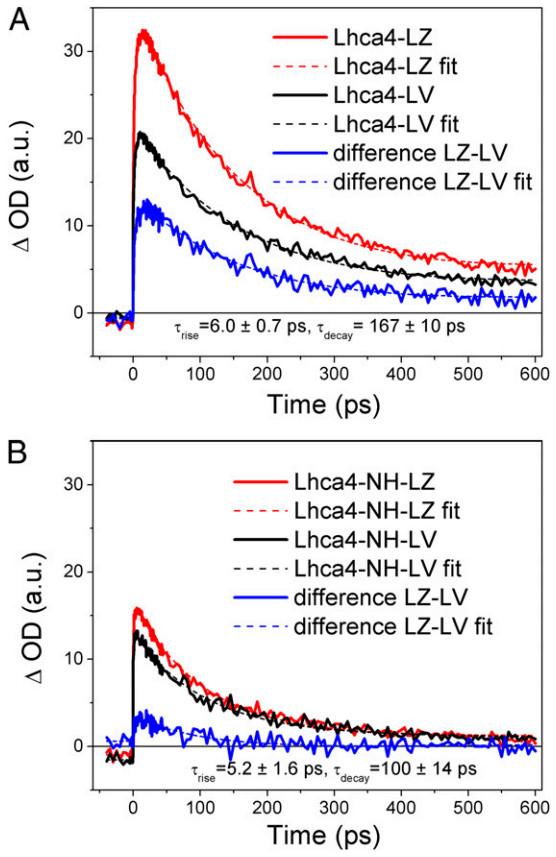

Fig. 6. Near IR transient absorption of Lhca4 complexes. Lhca4 WT and NH mutant binding lutein and violaxanthin (LV) or lutein and zeaxanthin (LZ) as carotenoids were used for pump (at 650 nm) and probe (at 980 nm) measurement. (*A*) Transient absorption kinetics of Lhca4 WT. (*B*) Transient absorption kinetics of Lhca4 NH mutants. The difference in kinetics (LZ minus LV) is shown in blue.

this reaction is enhanced by the tight interaction of chlorophyll 603 (A5) and chlorophyll 609 (B5) within the pigment–protein complex.

Discussion

In this work we show that zeaxanthin accumulation within the PSI–LHCI complex enhances photoprotection. In particular, upon light stress in vivo, the accumulation of zeaxanthin in the LHCI moiety of WT PSI–LHCI protects P700 activity as compared with PSI–LHCI from *npq1*, which lacks zeaxanthin (Fig. 1 and Fig. S1). This effect was confirmed by measuring both P700 activity and chlorophyll photobleaching in isolated PSI–LHCI complexes. Zeaxanthin in PSI–LHCI has been reported previously to enhance chlorophyll-triplet quenching in LHCI proteins, thus reducing the formation of singlet oxygen (62). Here, we show that zeaxanthin also down-regulates singlet chlorophyll excited states. The global analysis of the fluorescence decay kinetics of the PSI–LHCI supercomplex found decay components in violaxanthin-binding complexes to be basically in agreement with previous results (5, 6, 50, 51), whereas in presence of zeaxanthin we identified decay components reflecting a reduction of the trapping time of the absorbed excitation energy (Fig. 5). Moreover, although PSI-core decay kinetics remained unchanged in WT vs. *npq2* samples, with a major 13-ps decay component, the corresponding decay component in PSI–LHCI was slowed to 18 ps in the presence of violaxanthin in the LHCI complex. With zeaxanthin (in *npq2*), a 12-ps component was resolved, suggesting that energy transfer from LHCI to the PSI-core is reduced. The contribution of outer LHCI proteins in the PSI–LHCI supercomplex is most evident in the intermediate ~50-ps component. Here, the amplitude of red forms is clearly reduced by zeaxanthin (Fig. 4, and Fig. S6). In isolated LHCI proteins, however, the quenching effect of zeaxanthin is weak, and the fluorescence of both violaxanthin and zeaxanthin complexes decays mainly in nanoseconds. Thus, zeaxanthin-dependent quenching is most efficient when LHCI is connected with the PSI core. Zeaxanthin modifies the interaction between the PSI core and LHCI, causing switching from a light-harvesting state in which excitation energy is transferred efficiently to the PSI core, to a more dissipative state. This effect reduces the light-har-vesting capacity of PSI–LHCI by 30% (Fig. 2), and this reduction occurs within minutes after exposure to excess light without al-tering the stoichiometry between Lhca proteins and P700 (Fig. S4) (48). Zeaxanthin accumulates in PSI–LHCI complexes at the level of both LHCI subunits and the gap pigments (Table S2), as is consistent with the release of violaxanthin upon the dissocia-tion of LHCI from the PSI-core (49). The interaction between LHCI and the PSI-core increases the amplitude of the red spectral forms in the complex, suggesting that this effect is caused by a conformational change within Lhca proteins or by favoring interactions between gap pigments, or both. These two modes of action might prove difficult to distinguish because of the orientation of LHCI subunits within the supercomplex, with Chls 603 and 609 and binding site L2 (32) hosting zeaxanthin (20), facing the PSI core complex, located close to the gap chlorophylls, and likely acting as a bridge between the outer LHCI and the inner chlorophylls bound to PSI-core (4, 63). Thus, zeaxanthin accumulates in close proximity to the site by which excitation energy is transferred from LHCI to the PSI core (6, 64), increasing the strength of the red forms and slowing the migration time to the reaction center. The physiological role of red forms is still controversial in the absence of a mutant plant specifically lacking this feature. Red forms were associated with a charge-transfer state between chlorophyll 603 and chloro-phyll 609 (65), which was proposed exclude the formation of quenching states (60). This notion is consistent with our obser-vation that the 50-ps DAS from PSI–LHCI, dominated by LHCI, reduces its amplitude in red-shifted forms upon zeaxanthin binding. We suggest this reduction is caused the enhanced ac-tivity of a dissipative channel in LHCI efficiently connected to the PSI core. We also detected a LHCI subpopulation with longer lifetime (i.e., not in dissipative state) in which red forms are increased by zeaxanthin binding (Fig. 4 *A* and *B* and Fig. S6*C*), likely as the result of a stronger interaction between chlorophyll 603 and chlorophyll 609. This effect has been reported previously for the homologous protein Lhcb4 (59), but we cannot be sure if this population is present in vivo or if it arises from a tiny fraction of PSI–LHCI damaged during iso-lation and/or measurements. We interpret this result as evidence of the presence of multiple Lhca protein conformations among which we can identify at least four different protein states: (*i*) a light-harvesting state with a lifetime of nanoseconds, which leads to efficient energy transfer to P700 when Lhca proteins are bound to PSI (60); (*ii*) a zeaxanthin-dependent partially dissi-pative state with a lifetime of nanoseconds, as seen by comparing Lhca proteins in detergent with and without zeaxanthin (Fig. 4*D* and Table S4); this state cannot be observed in the PSI–LHCI supercomplex because it is quenched by P700 charge separation; (*iii*) a zeaxanthin- and red forms-independent dissipative state of ~200 ps identified in the protein in detergent, which again cannot be observed in the PSI–LHCI supercomplex because of P700 charge separation (60, 66); (*iv*) a zeaxanthin- and red forms-dependent highly dissipative conformation in which quenching is induced by the formation of a zeaxanthin radical cation with a formation time of a few picoseconds, a rate comparable to that of P700 charge separation. We propose that

this fourth dissipative state, detected in a subpopulation of zeaxanthin-binding Lhca4 in detergent (Fig. 6), is stabilized by the interaction of LHCI with PSI-core/gap pigments and is responsible for the zeaxanthin-dependent, 30%reduction of the functional antenna size in vivo. We cannot exclude the occurrence of other kind of zeaxanthin-dependent quenching mechanisms (67–69). The zeaxanthin-dependent reduction of functional PSI–LHCI antenna size is associated with improved photoprotection of PSI–LHCI both in vitro and in vivo. The need for zeaxanthin-dependent photoprotection mechanisms in PSI–LHCI likely is a consequence of the activity of Lhca proteins as "safety valves" and as primary targets of photoinhibition, according to a previous report (30). We conclude that, although both PSI and PSII undergo a photoprotective state that is dependent on zeaxanthin, the operation of the xanthophyll cycle is significantly different. Upon HL stress, PSII undergoes the most rapid response, consisting in the activation of NPQ; on a longer time scale LHCII migration to PSI–LHCI (state transition) is inhibited (70), thus reducing the size of the PSI–LHCI antenna. Zeaxanthin is accumulated in both photosystems, inducing multiple photoprotective effects including improved ^{3}Chl* quenching (62), ROS scavenging (71, 72), and a further reduction of light-harvesting activity in PSI (this work). In the long term (days), HL stress induces a reduction in PSII antenna size (50% in the case of *A. thaliana*) (13).

Materials and Methods

Plants Growth and Light Treatment. *A. thaliana* (Col-0) plants were grown for 4 wk at 100 $\mu E \cdot m^{-2} \cdot s^{-1}$, 19 °C, 90% humidity and 8 h of daylight. Photoinhibition treatment consisted in the illumination of plants with 2,000 $\mu E \cdot m^{-2} \cdot s^{-1}$ for 30 min and 90 min at 4 °C.

Measurement of P700 Activity. P700 activity was determined as P700 oxidation measured as a transient decrease in 705-nm absorption, as previously described (14). When P700 activity was measured on isolated PSI–LHCI complexes, 2 mM sodium ascorbate and 750 μM methyl-viologen (Sigma-Aldrich) were added to the sample.

Pigments Analysis. Pigments from leaves and isolated proteins were extracted in acetone 80% (Sigma-Aldrich) and analyzed by deconvolution of absorption spectra in the visible region and HPLC (Thermo-Fisher Scientific) separation as previously described (13).

PSI–LHCI, PSI-Core, and LHCI Isolation. PSI–LHCI was isolated from leaves as described in ref. 46 and 48. PSI-core and LHCI were isolated from PSI–LHCI samples as described in ref. 47.

Streak Camera Measurements. Time-resolved photoluminescence measurements were performed using a femtosecond laser source (Chameleon Ultra II, Coherent) and streak camera detection system (C5680, Hamamatsu) as described in ref. 73. Measurements of photoluminescence intensity as a function of both wavelength and time were obtained with spectral and temporal resolutions of ∼1 nm and ∼3 ps, respectively. Temporal broadening of the pump pulses caused by dispersive elements was confirmed to be well below the response time of the detection system. In the case of long-lifetime (>2 ns) measurements, an acousto-optic modulating pulse picker (APE Pulse Select) was used to reduce the oscillator repetition rate to 2 MHz, and a linear streak camera voltage sweep unit was used for detection, yielding temporal resolutions of ∼100 ps.

Global Analysis. The streak camera data were analyzed with software based on the approach described in ref. 53.

Protein Overexpression and Reconstitution. Lhca4 WT and NH mutant were overexpressed in *Escherichia coli*, purified, and refolded in vitro as described in ref. 74. During the reconstitution procedure, the added pigment mix contained either violaxanthin or zeaxanthin as described in ref. 59. In the violaxanthin-containing mix, pigments were extracted from spinach as described in ref. 74. For the zeaxanthin-binding complexes pigments were bought from Sigma-Aldrich.

Near IR Transient Absorption. Pump probe measurements were performed on Lhca4 complexes as described in ref. 59, with a 650-nm pump and a probe with femtosecond resolution at 980 nm.

ACKNOWLEDGMENTS. Research was funded in part through the European Union Seventh Framework Programme for Research Project 316427, Environmental Acclimation of Photosynthesis; the Italian Ministry of Agriculture, Food and Forestry Project HYDROBIO; the Italian Ministry for Education, Higher Education and Future Research Grant RBFR08XH0H; and by Woo Jang Chun Special Project PJ00910603201 financed by the Korean Rural Development Agency. This work was supported by the Director, Office of Science, Office of Basic Energy Sciences, of the US Department of Energy under Contract DE-AC02-05CH11231 and the Division of Chemical Sciences, Geosciences and Biosciences Division, Office of Basic Energy Sciences through Grant DE-AC03-76SF000098 (at Lawrence Berkeley National Laboratory and University of California, Berkeley).

1. Werst M, Jia Y, Mets L, Fleming GR (1992) Energy transfer and trapping in the photosystem I core antenna. A temperature study. *Biophys J* 61(4):868–878.
2. Croce R, Dorra D, Holzwarth AR, Jennings RC (2000) Fluorescence decay and spectral evolution in intact photosystem I of higher plants. *Biochemistry* 39(21): 6341–6348.
3. Jennings RC, Zucchelli G, Santabarbara S (2013) Photochemical trapping heterogeneity as a function of wavelength, in plant photosystem I (PSI-LHCI). *Biochim Biophys Acta* 1827(6):779–785.
4. Wientjes E, van Stokkum IH, van Amerongen H, Croce R (2011) Excitation-energy transfer dynamics of higher plant photosystem I light-harvesting complexes. *Biophys J* 100(5):1372–1380.
5. Slavov C, Ballottari M, Morosinotto T, Bassi R, Holzwarth AR (2008) Trap-limited charge separation kinetics in higher plant photosystem I complexes. *Biophys J* 94(9): 3601–3612.
6. Sener MK, et al. (2005) Comparison of the light-harvesting networks of plant and cyanobacterial photosystem I. *Biophys J* 89(3):1630–1642.
7. Caffarri S, Broess K, Croce R, van Amerongen H (2011) Excitation energy transfer and trapping in higher plant Photosystem II complexes with different antenna sizes. *Biophys J* 100(9):2094–2103.
8. Gilmore AM, Hazlett TL, Debrunner PG, Govindjee (1996) Photosystem II chlorophyll a fluorescence lifetimes and intensity are independent of the antenna size differences between barley wild-type and chlorina mutants: Photochemical quenching and xanthophyll cycle-dependent nonphotochemical quenching of fluorescence. *Photosynth Res* 48(1-2):171–187.
9. Roelofs TA, Lee CH, Holzwarth AR (1992) Global target analysis of picosecond chlorophyll fluorescence kinetics from pea chloroplasts: A new approach to the characterization of the primary processes in photosystem II alpha- and beta-units. *Biophys J* 61(5):1147–1163.
10. Ben-Shem A, Frolow F, Nelson N (2003) Crystal structure of plant photosystem I. *Nature* 426(6967):630–635.
11. Ferreira KN, Iverson TM, Maghlaoui K, Barber J, Iwata S (2004) Architecture of the photosynthetic oxygen-evolving center. *Science* 303(5665):1831–1838.
12. Caffarri S, Kouril R, Kereïche S, Boekema EJ, Croce R (2009) Functional architecture of higher plant photosystem II supercomplexes. *EMBO J* 28(19):3052–3063.
13. Ballottari M, Dall'Osto L, Morosinotto T, Bassi R (2007) Contrasting behavior of higher plant photosystem I and II antenna systems during acclimation. *J Biol Chem* 282(12): 8947–8958.
14. Bonente G, Pippa S, Castellano S, Bassi R, Ballottari M (2012) Acclimation of Chlamydomonas reinhardtii to different growth irradiances. *J Biol Chem* 287(8): 5833–5847.
15. Boekema EJ, van Roon H, Calkoen F, Bassi R, Dekker JP (1999) Multiple types of association of photosystem II and its light-harvesting antenna in partially solubilized photosystem II membranes. *Biochemistry* 38(8):2233–2239.
16. Niyogi KK (1999) Photoprotection revisited: Genetic and molecular approaches. *Annu Rev Plant Physiol Plant Mol Biol* 50:333–359.
17. Arnoux P, Morosinotto T, Saga G, Bassi R, Pignol D (2009) A structural basis for the pH-dependent xanthophyll cycle in Arabidopsis thaliana. *Plant Cell* 21(7):2036–2044.
18. Havaux M, Niyogi KK (1999) The violaxanthin cycle protects plants from photooxidative damage by more than one mechanism. *Proc Natl Acad Sci USA* 96(15): 8762–8767.
19. Horton P, Ruban AV, Wentworth M (2000) Allosteric regulation of the light-harvesting system of photosystem II. *Philos Trans R Soc Lond B Biol Sci* 355(1402): 1361–1370.
20. Wehner A, Storf S, Jahns P, Schmid VH (2004) De-epoxidation of violaxanthin in light-harvesting complex I proteins. *J Biol Chem* 279(26):26823–26829.
21. Jeong SW, et al. (2002) Differential susceptibility of photosynthesis to light-chilling stress in rice (Oryza sativa l.) depends on the capacity for photochemical dissipation of light. *Mol Cells* 13(3):419–428.
22. Bukhov NG, Govindachary S, Rajagopal S, Joly D, Carpentier R (2004) Enhanced rates of P700(+) dark-reduction in leaves of Cucumis sativus L photoinhibited at chilling temperature. *Planta* 218(5):852–861.
23. Tjus SE, Møller BL, Scheller HV (1998) Photosystem I is an early target of photoinhibition in barley illuminated at chilling temperatures. *Plant Physiol* 116(2):755–764.
24. Hui Y, Jie W, Carpentier R (2000) Degradation of the photosystem I complex during photoinhibition. *Photochem Photobiol* 72(4):508–512.

25. Kudoh H, Sonoike K (2002) Irreversible damage to photosystem I by chilling in the light: Cause of the degradation of chlorophyll after returning to normal growth temperature. *Planta* 215(4):541–548.
26. Velitchkova M, Yruela I, Alfonso M, Alonso PJ, Picorel R (2003) Different kinetics of photoinactivation of photosystem I-mediated electron transport and P700 in isolated thylakoid membranes. *J Photochem Photobiol B* 69(1):41–48.
27. Zhang S, Scheller HV (2004) Photoinhibition of photosystem I at chilling temperature and subsequent recovery in Arabidopsis thaliana. *Plant Cell Physiol* 45(11):1595–1602.
28. Oh MH, et al. (2009) Loss of peripheral polypeptides in the stromal side of photosystem I by light-chilling in cucumber leaves. *Photochem Photobiol Sci* 8(4):535–541.
29. Sonoike K (2011) Photoinhibition of photosystem I. *Physiol Plant* 142(1):56–64.
30. Alboresi A, Ballottari M, Hienerwadel R, Giacometti GM, Morosinotto T (2009) Antenna complexes protect Photosystem I from photoinhibition. *BMC Plant Biol* 9:71.
31. Caffarri S, Croce R, Breton J, Bassi R (2001) The major antenna complex of photosystem II has a xanthophyll binding site not involved in light harvesting. *J Biol Chem* 276(38):35924–35933.
32. Liu Z, et al. (2004) Crystal structure of spinach major light-harvesting complex at 2.72 A resolution. *Nature* 428(6980):287–292.
33. Standfuss J, Terwisscha van Scheltinga AC, Lamborghini M, Kühlbrandt W (2005) Mechanisms of photoprotection and nonphotochemical quenching in pea light-harvesting complex at 2.5 A resolution. *EMBO J* 24(5):919–928.
34. Pan X, et al. (2011) Structural insights into energy regulation of light-harvesting complex CP29 from spinach. *Nat Struct Mol Biol* 18(3):309–315.
35. Croce R, Weiss S, Bassi R (1999) Carotenoid-binding sites of the major light-harvesting complex II of higher plants. *J Biol Chem* 274(42):29613–29623.
36. Morosinotto T, Baronio R, Bassi R (2002) Dynamics of chromophore binding to Lhc proteins in vivo and in vitro during operation of the xanthophyll cycle. *J Biol Chem* 277(40):36913–36920.
37. Jahns P, Wehner A, Paulsen H, Hobe S (2001) De-epoxidation of violaxanthin after reconstitution into different carotenoid binding sites of light-harvesting complex II. *J Biol Chem* 276(25):22154–22159.
38. Betterle N, Ballottari M, Hienerwadel R, Dall'Osto L, Bassi R (2010) Dynamics of zeaxanthin binding to the photosystem II monomeric antenna protein Lhcb6 (CP24) and modulation of its photoprotection properties. *Arch Biochem Biophys* 504(1): 67–77.
39. Guliaev BA, Kukarskikh GP, Timofeev KN, Krendeleva TE (1979) [Photochemical and spectral properies of the photosystem I reaction centers-enriched particles]. *Biokhimiia* 44(3):564–569.
40. Croce R, Morosinotto T, Castelletti S, Breton J, Bassi R (2002) The Lhca antenna complexes of higher plants photosystem I. *Biochim Biophys Acta* 1556(1):29–40.
41. Morosinotto T, Breton J, Bassi R, Croce R (2003) The nature of a chlorophyll ligand in Lhca proteins determines the far red fluorescence emission typical of photosystem I. *J Biol Chem* 278(49):49223–49229.
42. Croce R, et al. (2004) Origin of the 701-nm fluorescence emission of the Lhca2 subunit of higher plant photosystem I. *J Biol Chem* 279(47):48543–48549.
43. Joliot P, Johnson GN (2011) Regulation of cyclic and linear electron flow in higher plants. *Proc Natl Acad Sci USA* 108(32):13317–13322.
44. Niyogi KK, Grossman AR, Björkman O (1998) Arabidopsis mutants define a central role for the xanthophyll cycle in the regulation of photosynthetic energy conversion. *Plant Cell* 10(7):1121–1134.
45. Dall'Osto L, Cazzaniga S, North H, Marion-Poll A, Bassi R (2007) The Arabidopsis aba4-1 mutant reveals a specific function for neoxanthin in protection against photooxidative stress. *Plant Cell* 19(3):1048–1064.
46. Croce R, Zucchelli G, Garlaschi FM, Bassi R, Jennings RC (1996) Excited state equilibration in the photosystem I-light-harvesting I complex: P700 is almost isoenergetic with its antenna. *Biochemistry* 35(26):8572–8579.
47. Croce R, Zucchelli G, Garlaschi FM, Jennings RC (1998) A thermal broadening study of the antenna chlorophylls in PSI-200, LHCI, and PSI core. *Biochemistry* 37(50): 17355–17360.
48. Ballottari M, Govoni C, Caffarri S, Morosinotto T (2004) Stoichiometry of LHCI antenna polypeptides and characterization of gap and linker pigments in higher plants Photosystem I. *Eur J Biochem* 271(23-24):4659–4665.
49. Morosinotto T, Ballottari M, Klimmek F, Jansson S, Bassi R (2005) The association of the antenna system to photosystem I in higher plants. Cooperative interactions stabilize the supramolecular complex and enhance red-shifted spectral forms. *J Biol Chem* 280(35):31050–31058.
50. Ihalainen JA, et al. (2002) Pigment organization and energy transfer dynamics in isolated photosystem I (PSI) complexes from Arabidopsis thaliana depleted of the PSI-G, PSI-K, PSI-L, or PSI-N subunit. *Biophys J* 83(4):2190–2201.
51. Wientjes E, van Stokkum IH, van Amerongen H, Croce R (2011) The role of the individual Lhcas in photosystem I excitation energy trapping. *Biophys J* 101(3):745–754.
52. Galka P, et al. (2012) Functional analyses of the plant photosystem I-light-harvesting complex II supercomplex reveal that light-harvesting complex II loosely bound to photosystem II is a very efficient antenna for photosystem I in state II. *Plant Cell* 24(7): 2963–2978.
53. van Stokkum IH, Larsen DS, van Grondelle R (2004) Global and target analysis of time-resolved spectra. *Biochim Biophys Acta* 1657(2-3):82–104.
54. Holzwarth AR, Schatz G, Brock H, Bittersmann E (1993) Energy transfer and charge separation kinetics in photosystem I: Part 1: Picosecond transient absorption and fluorescence study of cyanobacterial photosystem I particles. *Biophys J* 64(6):1813–1826.
55. Croce R, van Amerongen H (2013) Light-harvesting in photosystem I. *Photosynth Res* 116:153–166.
56. Wientjes E, Oostergetel GT, Jansson S, Boekema EJ, Croce R (2009) The role of Lhca complexes in the supramolecular organization of higher plant photosystem I. *J Biol Chem* 284(12):7803–7810.
57. Moya I, Silvestri M, Vallon O, Cinque G, Bassi R (2001) Time-resolved fluorescence analysis of the photosystem II antenna proteins in detergent micelles and liposomes. *Biochemistry* 40(42):12552–12561.
58. Krüger TP, Wientjes E, Croce R, van Grondelle R (2011) Conformational switching explains the intrinsic multifunctionality of plant light-harvesting complexes. *Proc Natl Acad Sci USA* 108(33):13516–13521.
59. Ahn TK, et al. (2008) Architecture of a charge-transfer state regulating light harvesting in a plant antenna protein. *Science* 320(5877):794–797.
60. Passarini F, Wientjes E, van Amerongen H, Croce R (2010) Photosystem I light-harvesting complex Lhca4 adopts multiple conformations: Red forms and excited-state quenching are mutually exclusive. *Biochim Biophys Acta* 1797(4):501–508.
61. Holt NE, et al. (2005) Carotenoid cation formation and the regulation of photosynthetic light harvesting. *Science* 307(5708):433–436.
62. Dall'Osto L, et al. (2012) Zeaxanthin protects plant photosynthesis by modulating chlorophyll triplet yield in specific light-harvesting antenna subunits. *J Biol Chem* 287(50):41820–41834.
63. Jennings RC, Garlaschi FM, Zucchelli G (2003) Excited state trapping and the Stepanov relation with reference to Photosystem I. *Biophys J* 85(6):3923–3927.
64. Ihalainen JA, et al. (2005) Excitation energy trapping in photosystem I complexes depleted in Lhca1 and Lhca4. *FEBS Lett* 579(21):4787–4791.
65. Romero E, et al. (2009) The origin of the low-energy form of photosystem I light-harvesting complex Lhca4: Mixing of the lowest exciton with a charge-transfer state. *Biophys J* 96(5):L35–L37.
66. Wientjes E, Roest G, Croce R (2012) From red to blue to far-red in Lhca4: How does the protein modulate the spectral properties of the pigments? *Biochim Biophys Acta* 1817(5):711–717.
67. Fuciman M, et al. (2012) Role of xanthophylls in light harvesting in green plants: A spectroscopic investigation of mutant LHCII and Lhcb pigment-protein complexes. *J Phys Chem B* 116(12):3834–3849.
68. Liao PN, Holleboom CP, Wilk L, Kühlbrandt W, Walla PJ (2010) Correlation of Car S(1) → Chl with Chl → Car S(1) energy transfer supports the excitonic model in quenched light harvesting complex II. *J Phys Chem B* 114(47):15650–15655.
69. Polívka T, et al. (2002) Carotenoid S(1) state in a recombinant light-harvesting complex of Photosystem II. *Biochemistry* 41(2):439–450.
70. Pesaresi P, et al. (2010) Optimizing photosynthesis under fluctuating light: The role of the Arabidopsis STN7 kinase. *Plant Signal Behav* 5(1):21–25.
71. Dall'Osto L, Cazzaniga S, Havaux M, Bassi R (2010) Enhanced photoprotection by protein-bound vs free xanthophyll pools: A comparative analysis of chlorophyll b and xanthophyll biosynthesis mutants. *Mol Plant* 3(3):576–593.
72. Baroli I, Do AD, Yamane T, Niyogi KK (2003) Zeaxanthin accumulation in the absence of a functional xanthophyll cycle protects Chlamydomonas reinhardtii from photooxidative stress. *Plant Cell* 15(4):992–1008.
73. Cesaratto A, et al. (2014) Analysis of cadmium-based pigments with time-resolved photoluminescence. *Anal. Methods* 6:130–138.
74. Giuffra E, Cugini D, Croce R, Bassi R (1996) Reconstitution and pigment-binding properties of recombinant CP29. *Eur J Biochem* 238(1):112–120.